*% detected as AI

AI detection includes the possibility of false positives. Although some text in this submission is likely AI generated, scores below the 20% threshold are not surfaced because they have a higher likelihood of false positives.

Caution: Review required.

It is essential to understand the limitations of AI detection before making decisions about a student's work. We encourage you to learn more about Turnitin's AI detection capabilities before using the tool.

Disclaimer

Our AI writing assessment is designed to help educators identify text that might be prepared by a generative AI tool. Our AI writing assessment may not always be accurate (it may misidentify writing that is likely human generated as AI generated and likely AI generated as human generated) so it should not be used as the sole basis for adverse actions against a student. It takes further scrutiny and human judgment in conjunction with an organization's application of its specific academic policies to determine whether any academic misconduct has occurred.

Development of Nanofiller-Reinforced Polymeric Adhesives Combined with an Acrylic Copolymer for Archaeological Stone Restoration

Israa Abdulsatar Ismael[1] Faris Muayed Ahmed[1] , Omer A. Alwash[1]*, Luma J. hamoody[1], Nadia Fakhry Ibraheem[1]

[1]Scientific Research Commission, Baghdad, Iraq

*Corresponding author: omar.a.abdulameer@src.edu.iq

Abstract

Epoxy resin and polyvinyl acetate adhesives are widely used to treat cracks and fractures in stone antiquities. This study describes the development, mechanical evaluation, and application of high-performance epoxy resin and polyvinyl acetate (PVAc) adhesives reinforced with inorganic fillers, specifically engineered for archaeological stone restoration. The epoxy resin was reinforced with silica nanoparticles (SiO_2, ~50 nm) and zinc oxide nanoparticles (ZnO, ~50 nm) at two loading levels: 2 wt% SiO_2 + 2 wt% ZnO and 5 wt% SiO_2 + 5 wt% ZnO. Similarly, PVAc was reinforced with the same proportions of both additives. An acrylic copolymer (Paraloid B-72) was applied as a barrier coating to the stone surface before adhesive application. This intervening barrier protects the original substrate by preventing direct contact between the adhesive and the artifact. Consequently, if adhesive removal becomes necessary, the solvent-removable coating is intended to facilitate separation while minimizing the risk of damage to the underlying archaeological stone. The epoxy composite containing 5% nano-SiO_2 and 5% ZnO exhibited the highest shear strength (46.94 MPa), whereas the corresponding PVAc composite achieved 35.90 MPa. At the lower nanoparticle loading, the epoxy composite containing 2% nano-SiO_2 and 2% ZnO achieved a maximum shear strength of 39.99 MPa, compared with 17.289 MPa for the corresponding PVAc composite. Fourier-transform infrared (FTIR) spectroscopy was used to characterize the adhesive formulations, whereas XRF was used to determine the elemental composition of the limestone and marble samples.

Keywords: archaeological restoration; polymeric adhesives; nanoparticles; acrylic copolymer

1. Introduction

Iraq possesses an extremely rich archaeological heritage, comprising thousands of artifacts made of stone, ceramics, and metal. These materials are vulnerable to biological deterioration and to damage caused by environmental conditions, transportation, storage, and armed conflicts. Consequently, reliable restoration materials, including polymeric adhesives, are essential for ensuring the structural stability of artifacts while preserving their historical authenticity (1). Polymeric adhesives address evolving needs in industries ranging from aerospace and automotive engineering to construction (2). They offer a combination of properties, including a high strength-to-weight ratio, excellent thermal and corrosion resistance, stability, and flexibility, making them suitable for diverse applications in critical sectors (3–5). Adhesives are used to join solid surfaces, whereas adhesion is the interfacial process that enables load transfer between bonded substrates (6). Adhesion involves intimate contact between two substrates, allowing mechanical forces to be transferred across the interface and through the bonded joint (7). Adhesives are used to bond materials such as metal, paper, and stone, and to reassemble fractured artifacts and statues damaged by weather, environmental fluctuations, impact, or accidental falls (8).

Epoxy resin is among the most widely used structural adhesives for stone conservation and the reassembly of fractured stone because of its outstanding mechanical properties (9), chemical and moisture resistance, and long-term durability (10). It has been successfully employed to reconstruct fractured stone, ceramic, and metallic artifacts. However, the irreversibility of cured epoxy and the difficulty of its removal are significant limitations (11). Its strong adhesion is associated with polar functional groups, including hydroxyl and ether groups, which contribute to interfacial interactions and the mechanical performance of the cured material (12). Since polymers began to be widely used to consolidate decayed stone in the 1960s, epoxy materials have attracted considerable interest as stone adhesives and gap fillers because of their mechanical strength, durability, and exceptional adhesion (13–15). Epoxy formulations are used for applications requiring high mechanical performance, including the bonding of marble and granite; depending on their formulation and viscosity, they may also be applied as coatings (16–17). Polyvinyl acetate (PVAc) is another adhesive frequently used in restoration because of its ease of application, flexibility, and comparatively greater reversibility than epoxy adhesives. It also exhibits good compatibility with various archaeological materials (18). Nevertheless, its lower mechanical strength and limited moisture resistance restrict its use in demanding conservation environments (19). Its principal advantages include ease of application, flexibility, availability, low cost, and reported resistance to aging and biological attack (20). Fillers can occupy spaces within a polymer matrix and enhance the strength, durability, and hardness of the resulting product (21). Stone materials were used to produce statues, obelisks, and panels. Limestone, which occurs in Iraqi antiquities, is composed principally of calcium carbonate and may also contain silica, iron oxides, and small amounts of magnesium carbonate (22–23); its color is typically white or yellowish. Marble is a metamorphic rock derived from carbonate rocks such as limestone and consists predominantly of calcite and/or dolomite, with accessory minerals depending on the source rock (24–25). Nanomaterials have considerable

potential to enhance the performance and functionality of composites in diverse industrial applications (26). They have been used to improve polymer durability and thermal, physical, and mechanical performance, including hardness and bond strength (27). Their small size, high specific surface area, and high surface energy can enhance physical and chemical interactions and interfacial bonding between a polymer matrix and its reinforcement (28). Previous studies have examined inorganic nanofillers such as silicon dioxide (SiO_2) in polymer systems for conservation applications and have reported that particle size can affect mechanical properties, including hardness and toughness (29). Nanotechnology has numerous applications, including the preparation of epoxy- and PVAc-based adhesives (30–31). Zinc oxide is one of the most widely investigated nanomaterials for cultural heritage conservation because of its UV-shielding capacity, thermal stability, antimicrobial activity, and potential to enhance the mechanical performance of polymeric adhesives (32). When incorporated into polymeric systems such as epoxy and PVAc, ZnO nanoparticles have been reported to improve selected functional properties (33–36). Protecting the original surface of an archaeological artifact is a fundamental principle of conservation practice (37). Acrylic copolymers, particularly Paraloid B-72, are therefore widely used in conservation, although other formulations, including Paraloid B-67, B-44, and B-66, are also available (38). Paraloid B-72 reportedly does not discolor the surface when used for consolidation and is therefore considered suitable for cultural heritage preservation (39). It may also increase the water resistance of artifact surfaces (40) and is widely used as a removable barrier layer between an artifact surface and a structural adhesive (41). This protective layer prevents direct adhesion to the original substrate and can reduce the risk of damage during lifting, transportation, and conservation procedures (42). Acrylic polymers used in surface coatings or adhesives can be removed using solvents such as acetone and methyl ethyl ketone (43). Although several studies have investigated epoxy or PVAc modified with individual nanoparticles such as SiO_2 or ZnO, limited research has explored the combined incorporation of both nanoparticles into the same adhesive system for archaeological conservation. Comparative studies evaluating epoxy and PVAc reinforced with SiO_2 and ZnO nanoparticles under identical conditions are also scarce. Furthermore, the use of Paraloid B-72 as a removable isolation layer before adhesive bonding has not been comprehensively evaluated. This study therefore seeks to address these gaps by developing nanoparticle-reinforced adhesive systems that combine high mechanical performance and durability with the reversibility and compatibility required for cultural heritage conservation.

This study aimed to develop and evaluate epoxy- and PVAc-based adhesive systems reinforced with silicon dioxide and zinc oxide nanoparticles, with Paraloid B-72 used as a removable barrier layer. The objectives were to improve bond, shear, tensile, and slip-resistance performance while protecting the artifact substrate and to assess the potential of these systems for repairing cracks and fractures in stone pieces of different sizes and types.

4

2. Experimental Part

2.1. Chemicals

2.1.1. Conbextra EP10 epoxy resin (Fosroc, Jordan), based on diglycidyl ether of bisphenol A (DGEBA), was used, as shown in Fig. 1 (44). The resin and ethylenediamine hardener were mixed at a 3:1 ratio. The resin had a density of 1,050 kg/m³ and a viscosity of 150–200 cP at 25 °C.

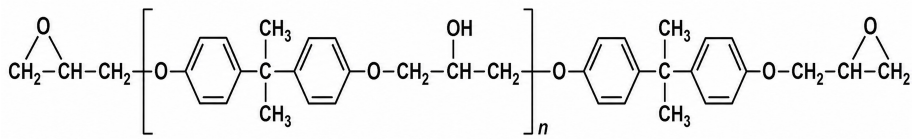

Fig. 1. Chemical structure of the epoxy resin.

2.1.2. Polyvinyl acetate adhesive was obtained from Abnilshimi Company, Islamic Republic of Iran. The PVAc adhesive was supplied as an emulsion with a viscosity of 29,000–30,000 cP, a density of 1.30–1.35 g/cm³, a solids content of 59%, and a pH of 9. PVAc is widely used in waterborne adhesive formulations and polymer films because of its low cost, excellent adhesion to polar substrates, ease of processing, and low toxicity. Its molecular formula is $(C_4H_6O_2)_n$, and its repeating unit is $[–CH_2–CH(OCOCH_3)–]_n$ (45).

2.1.3. Paraloid B-72 (Acraloid B-72) is an acrylic copolymer composed of ethyl methacrylate (70%) and methyl acrylate (30%) monomers (EMA/MA) (Aldrich, Darmstadt, Germany), as shown in Fig. 2. It has a density of 1.15 g/cm³ and a refractive index of 1.479–1.489 and was supplied as transparent granules (46). It was dissolved in acetone or methyl ethyl ketone to prepare a primer coating for the stone surface.

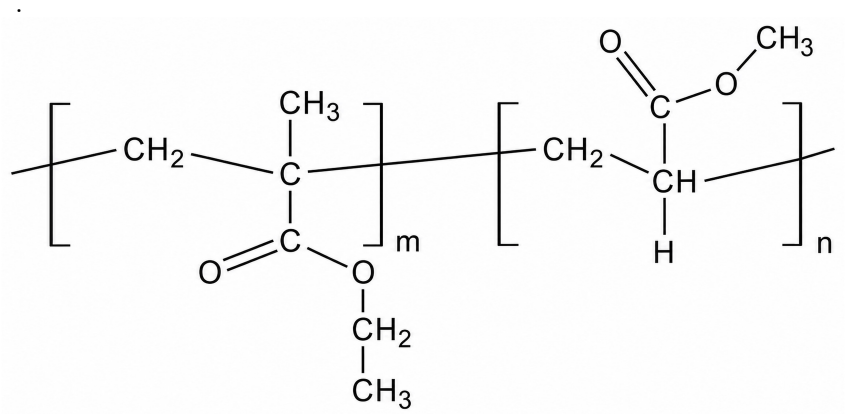

Fig. 2. Chemical structure of Paraloid B-72.

5

2.1.4. The inorganic nanofillers were nano-SiO_2 and ZnO nanoparticles, each with a nominal particle size of 50 nm. The nanofillers had a reported purity of 99.7% and a bulk density of 0.3–0.5 g/mL (47).

2.2. Materials

Preparation of Experimental Limestone Samples

Experimental limestone blocks were cut into rectangular specimens measuring 10 × 2 × 2 cm for tensile-strength testing. Specimens measuring 75 × 75 mm were prepared for bond-strength testing, and specimens measuring 12 × 12 mm were prepared for slip-resistance testing (48). Before the nanocomposite adhesives were applied, the specimens were cleaned with a soft brush, washed with distilled water, and dried in an oven at 100 °C.

2.3. Methodologies

2.3.1. Preparation of Nanocomposite Adhesives

Nanoparticles were dispersed in the epoxy resin to obtain nanocomposites with the most homogeneous filler distribution possible (49–50). Epoxy nanocomposites are typically prepared by first dispersing the nanoparticles in the epoxy component before the hardener is added (51). SiO_2 and ZnO nanoparticles were incorporated into the epoxy resin at two loading levels: 2 wt% SiO_2 + 2 wt% ZnO (sample 2) and 5 wt% SiO_2 + 5 wt% ZnO (sample 3). Each formulation was initially mixed with a glass rod and then mechanically stirred at 500 rpm for 1 h to promote nanoparticle dispersion and minimize agglomeration. Finally, the hardener was added to each formulation at a resin-to-hardener ratio of 3:1.

2.3.2. Preparation of Epoxy- and PVAc-Nanoparticle Samples

Sample 1 consisted of epoxy resin and hardener mixed at a ratio of 3:1.

Sample 2 consisted of epoxy resin containing 2 wt% SiO_2 and 2 wt% ZnO (nominal particle size: 50 nm), mixed with hardener at a ratio of 3:1.

Sample 3 consisted of epoxy resin containing 5 wt% SiO_2 and 5 wt% ZnO (nominal particle size: 50 nm), mixed with hardener at a ratio of 3:1.

Sample 4 consisted of neat PVAc.

Sample 5 consisted of PVAc containing 2 wt% SiO_2 and 2 wt% ZnO.

Sample 6 consisted of PVAc containing 5 wt% SiO_2 and 5 wt% ZnO.

Sample 7 consisted of a 50% Paraloid B-72 solution in acetone. The solution was allowed to dissolve for 24 h, applied to the stone surface as a coating, and allowed to dry for 3–5 min (52).

2.3.3. Scanning Electron Microscopy (SEM)

SEM images of nano-SiO_2 with an average particle size of approximately 50 nm were obtained, as shown in Fig. 3 (53). SEM analysis was performed at the Nanotechnology Laboratory, Centre for Industrial Applications Research and Materials Technology, Scientific Research Commission, Baghdad, Iraq.

6

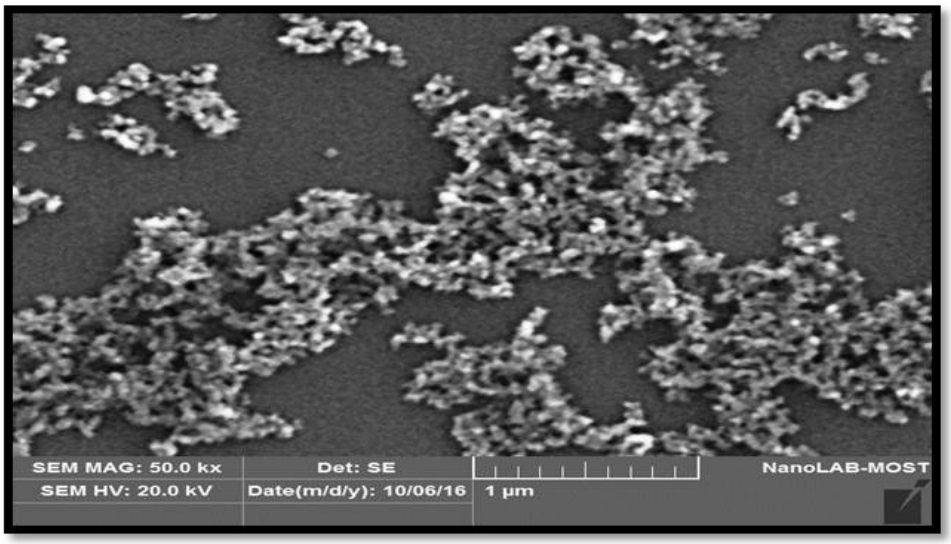

Fig. 3. Scanning electron microscopy (SEM) image of nano-SiO_2.

2.3.4. Preparation of Bonded Experimental Limestone Specimens

A. Two chemically modified limestone blocks were prepared in accordance with ASTM C321-00 (reapproved 2005). This standard method uses a compression-testing machine to measure the bond strength of the prepared polymeric adhesives. Paraloid B-72 was applied to the 75 × 75 mm joint area between the two blocks as a barrier coating. A 2–3 mm layer was applied and allowed to dry for 3–5 min. The polymeric adhesive was then applied over the same area at the same thickness and allowed to cure for at least 7 days for epoxy resin or dry for 3 days for PVAc (54–55). Adhesive testing was conducted at the Cement Laboratory, Building Research Centre, Baghdad, Iraq. Bond strength was calculated using Eq. (1).

$$\sigma_b = L/J \quad (1)$$

J = joint area between the adhesive and mortar (75 × 75 mm²)

L = maximum applied load (N)

σ_b = bond strength (MPa or N/mm²)

B. Limestone specimens measuring 12 × 12 mm were used to evaluate slip resistance. The adhesive was applied under normal laboratory conditions at a thickness of 2–3 mm. Each stone was then fixed to a vertical wall without additional support, and the interval between adhesive application and stone placement did not exceed 5 min (56). Vertical displacement was subsequently assessed in accordance with Iraqi Standard Specification MQA 1476/1992.

C. Stone samples were finely ground and pressed into circular discs, as shown in Fig. 4, and analyzed using a SPECTRO XEPOS X-ray fluorescence (XRF)

spectrometer. XRF was used to determine the concentrations and types of elements and oxides present in stones used in restoration and construction, including stone materials in Iraqi museums (57). The analysis was performed at the XRF Laboratory, Centre for Industrial Applications Research and Materials Technology, Scientific Research Commission, Baghdad, Iraq. Oxide percentages were calculated from elemental concentrations using Eq. (2).

Oxide (%) = Element (%) × Stoichiometric factor (2)

Stoichiometric factor = molar mass of the oxide/molar mass of the element

Fig. 4. Circular disc prepared from a stone sample.

2.3.5. Laboratory Testing

The prepared adhesives and bonded experimental limestone specimens were subjected to two accelerated-weathering protocols, as follows:

A. Salt-crystallization weathering

The experimental specimens were subjected to five salt-crystallization cycles. Each cycle consisted of immersion in saturated Na_2SO_4 for 5 h, exposure to air at 25 °C and 50% relative humidity for 30 h, and oven drying at 70 °C for 16 h (58).

B. Water-immersion weathering. Water-immersion testing was used to evaluate the resistance of the prepared adhesives to water and moisture when bonding stone pieces. The specimens underwent 20 immersion–drying cycles, each consisting of complete immersion in distilled water for 6 h followed by oven drying at 70 °C for 4 h (59). This protocol was intended to assess whether bonded stone pieces could tolerate washing when surface salts appear, as may occur in museum conservation practice.

8

3. Characterization

The mechanical properties of the nanocomposite adhesives were evaluated using the following mechanical and physicochemical characterization methods.

3.1. Bond-strength testing was performed using a universal/compression-testing machine in accordance with the stated procedure (ST-con.12) and ASTM C321-00 (reapproved 2005), a standard method for measuring bond strength (60).

3.2. Shear Strength. Shear strength is the maximum shear stress sustained by a specimen before failure (61). It was measured using a CESH-001.TSQ-1 H50KT testing machine (UK) in accordance with Ministry of Industry and Trade Standard Specification No. 1476/1992 and calculated using Eq. (3).

$$\tau_u = Fmax/A_s \quad (3)$$

τ_u = ultimate shear strength (MPa or N/mm²)

Fmax = maximum load at failure (N)

A_s = shear area (mm²)

3.3. Tensile Strength. Tensile strength (MPa or N/mm²) is the maximum tensile stress that a material can withstand before fracture or failure (62). It was measured using a Tinius Olsen H50KT testing machine (UK) at a crosshead speed of 10 mm/min in accordance with ASTM D638-89 and calculated using Eq. (4).

$$\sigma UTS = Fmax/A_o \quad (4)$$

σUTS = ultimate tensile strength (MPa or N/mm²)

Fmax = maximum tensile load applied before fracture (N)

A_o = original cross-sectional area of the specimen (mm²)

Adhesive specimens were prepared in the standard dumbbell shape specified in ASTM D638-89, as shown in Fig. 5.

Fig. 5. Standard dumbbell-shaped adhesive specimen.

3.4. Compressive Strength. Compressive strength was determined by subjecting each specimen to axial compression using a Tinius Olsen H50KT testing machine (63) and was calculated using Eq. (5).

$$\sigma UCS = Fmax/A_o \quad (5)$$

σUCS = ultimate compressive strength (MPa or N/mm²)

Fmax = maximum compressive load applied before failure (N)

A_o = original cross-sectional area of the specimen (mm²)

Cylindrical adhesive specimens (50 mm in diameter and 100 mm in height) were prepared in accordance with ASTM C579. Compressive-strength testing was performed at the Materials Laboratory, Centre for Industrial Applications Research and Materials Technology, Scientific Research Commission, Baghdad, Iraq.

3.5. X-ray Fluorescence. X-ray fluorescence (XRF) spectroscopy was used to determine the concentrations and types of elements in the stone specimens by measuring the characteristic X-rays emitted following excitation (64).

3.6. Slip Resistance. Slip resistance is a fundamental physical–mechanical property of adhesives used in vertical applications, such as fixing stone to walls and façades. It describes the ability of an uncured adhesive to prevent a stone from moving downward under its own weight before the adhesive develops its final bond strength.

Slip resistance depends on several factors:

A. Apparent viscosity: a higher apparent viscosity generally increases slip resistance.

B. Initial yield stress: a higher minimum of shear stress required to initiate adhesive flow generally helps resist sagging or slip before setting.

C. Bond-line thickness: thinner adhesive layers generally reduce the tendency to slip.

3.7. Curing and Drying Times. Epoxy curing time is the period during which the resin–hardener reaction develops a crosslinked network. In contrast, the drying time of a PVAc emulsion is governed primarily by water loss and film formation.

3.8. Fourier-Transform Infrared Spectroscopy. FTIR spectra were recorded for all epoxy and PVAc samples using the KBr-pellet method on a Shimadzu FTIR-8300 instrument over the range 400–4,000 cm^{-1} (64). The measurements were performed at the FTIR Laboratory, Centre for Industrial Applications Research and Materials Technology, Scientific Research Commission, Baghdad, Iraq.

4. Results and Discussion

4.1. Bond Strength

The prepared adhesives (samples 1–7) were investigated, as shown in Table 1. The neat epoxy adhesive bonded to the stone specimens exhibited a bond strength of 30.481 N/mm^2. However, the addition of nanomaterials to the epoxy produced higher bond strengths of 45.519 N/mm^2 for the epoxy adhesive containing 5% silicon dioxide and 5% zinc oxide nanoparticles and 40.441 N/mm^2 for that containing 2% silicon dioxide and 2% zinc oxide nanoparticles. This improvement is attributed to the synergistic effect of the combined nanomaterials. They form a single, cohesive network capable of distributing compressive loads over a larger area, increasing the bond strength from 30.481 N/mm^2 to 40.441 and 45.519 N/mm^2, respectively. Silicon dioxide (SiO_2) provides structural rigidity and a load-bearing network, whereas zinc oxide (ZnO) provides chemical adhesion and environmental protection. When combined at the 2% and 5% ratios, they produce strong, cohesive, and durable adhesives. The nanoparticle-reinforced epoxy can withstand high mechanical loads, making the newly prepared formulations suitable for restoring large and medium-sized stone fragments in archaeological and architectural applications (65). The bond-strength values of the PVAc formulations containing 5% and 2% nanoparticles were 25.244 and 18.318 N/mm^2, respectively, whereas neat PVAc exhibited a bond strength of 10.10 N/mm^2. Although these values were lower than those obtained for epoxy, the

formulations were suitable for bonding small stones. Adding nano to PVAc enhances its properties (66). The increase in strength may be associated with nanoparticle reinforcement and improved interfacial load transfer. Paraloid B-72 was used as a pre-applied barrier coating rather than as a component of the adhesive mixtures.

4.2. Shear Strength

The results showed that adding SiO_2 and ZnO nanoparticles to epoxy resin improved its resistance to layer slippage. The shear strength increased from 30.057 MPa for neat epoxy to 39.99 MPa following the addition of 2% nano-SiO_2 and 2% ZnO and to 46.94 MPa following the addition of 5% nano-SiO_2 and 5% ZnO, as shown in Table 1. This improvement is attributed to the formation of a nanonetwork that inhibits the slippage of polymer chains, enhances chemical adhesion at the epoxy–stone contact surface, and fills voids that weaken shear strength (67). The shear strength of PVAc increased from 10.34 MPa for neat PVAc to 17.289 MPa and 35.90 MPa for the formulations containing 2% and 5% nanoparticles, respectively. Fig. 6 demonstrates a marked improvement in the force-extension curves as nanoparticle concentration increases. While the neat epoxy sample exhibited a relatively low peak force at a given extension, the curve peak rose substantially for the 5% sample, along with a noticeable increase in the steepness of the initial linear slope. This behavior reflects an enhancement in both the elastic modulus and the resistance to layer slippage. Such improvements are attributed to the ability of SiO2 and ZnO nanoparticles to construct a three-dimensional network that restricts mobility of polymer chains and delays the onset of plastic deformation. These results confirm the dual functionality of these nanoparticles in simultaneously improving both the stiffness and the ultimate shear strength.

4.3. Tensile Strength

The tensile strength results showed that adding zinc oxide (ZnO) and silicon dioxide (SiO_2) nanoparticles to epoxy increased its tensile strength. The tensile strength increased from 9.25 MPa for neat epoxy to 16.09 MPa for the formulation containing 2% nano-SiO_2 and 2% ZnO, as shown in Fig. 7, and to 20.4 MPa for the formulation containing 5% nano-SiO_2 and 5% ZnO. Tensile stress is the applied force divided by the original cross-sectional area, and failure occurs when the specimen can no longer sustain the applied stress. The improved tensile strength may be related to nanoparticle reinforcement, crack-path modification, and interfacial load transfer (68). The separate effects of ZnO and SiO_2 cannot be determined from the present combined-filler design. The tensile strength of neat PVAc was 8.2 MPa, whereas the formulations containing 2% nano-SiO_2 and 2% ZnO and 5% nano-SiO_2 and 5% ZnO achieved 11.21 and 13.21 MPa, respectively, as shown in Table 1 and Fig. 8.

4.4. Compressive Strength

The compressive-strength results showed that adding nanoparticles to epoxy progressively improved its compressive strength in proportion to the percentages used. The value increased from 56.3 MPa for neat epoxy to 67.3 MPa for the formulation containing 2% nano-SiO_2 and 2% ZnO and to 86.20 MPa for the

formulation containing 5% nano-SiO_2 and 5% ZnO, as shown in Table 1 and Fig. 9. This improvement is attributed to the formation of a nanonetwork at the 5% loading, which inhibits crack propagation, distributes stress, fills gaps, and enhances cohesion between the polymer chains (69–70). Therefore, this percentage is suitable for bonding large stones, whereas the 2% loading is suitable for bonding medium- and small-sized stones. The compressive strength of neat PVAc was 25.9 MPa, whereas the formulations containing 2% nano-SiO_2 and 2% ZnO and 5% nano-SiO_2 and 5% ZnO achieved 55.9 and 61.4 MPa, respectively, as shown in Table 1.

4.5. Slip Resistance

The slip-resistance test measures the time required for a stone to adhere to a vertical limestone or marble wall using an adhesive. A good adhesive is characterized by its ability to fix the stone and prevent slippage, thereby providing a high degree of stability and rapid adhesion without requiring additional support. This property helps the worker complete the bonding of stones and ancient statues quickly. The adhesives prepared in this study achieved this outcome. The PVAc nano adhesives containing 5% nano-SiO_2 and 5% ZnO and 2% nano-SiO_2 and 2% ZnO recorded a short fixing time of 2–3 min without slippage or additional support. Epoxy adhesive samples 1, 2, and 3 exhibited lower slip resistance, with a fixing time of 15 min, whereas Paraloid B-72 required approximately 5 min. All results are shown in Table 2.

4.6. Water-Immersion Testing

Water-immersion testing is important for determining the water and moisture resistance of prepared adhesives used to bond stone pieces. The test consisted of 20 immersion–drying cycles: 6 h of complete immersion in distilled water followed by 4 h in an oven at 70 °C. The results showed that the adhesives resisted water immersion and were neither affected nor dissolved. Consequently, the stone pieces can be washed when salt appears, as practiced in museums to remove salt from artifact surfaces.

4.7. Curing and Drying Times.

The curing time of epoxy is the period during which epoxy resin (A) reacts with hardener (B). For all epoxy-resin adhesives, the initial curing time ranged from 2 to 3 h, whereas the final curing time reached 7 days, depending on the laboratory temperature of 45 °C. The initial drying time of PVAc was 5–6 h for all formulations, whereas the final drying time was 3 days. The Paraloid B-72 isolation coating had an initial drying time of 1–2 h and a final drying time of 24 h, also depending on the laboratory temperature of 45 °C. All results are shown in Table 2.

4.8. X-ray Fluorescence Analysis.

XRF was used to determine the concentrations and types of elements present in the stones used in the bonding processes and in artifact stones, as shown in Figs. 10 and 11 and Table 3. The elemental weight percentages (wt.%) obtained by XRF were converted into oxide weight percentages (wt.%) as shown in Table 4 using internationally recognized stoichiometric factors (IUPAC standards). This conversion was performed to standardize the results with those of previous geological and archaeological studies and to comply with Iraqi Standard Specification MQA 1476/1992 for building and restoration materials. The XRF spectrum of the limestone and marble (Figs. 10,11), reveals a clear two distinct peaks; the first, at 0.45 keV, is attributed to the line of calcium (Ca), confirming that the primary component of the samples is calcium carbonate. The second prominent peak at 1.74 keV corresponds to silicon (Si), indicating the presence of silicate impurities (such as quartz or clay minerals) within the structure of the stones. Limestone recorded higher values of iron 0.1309% and manganese 0.0103% respectively, compared to marble 0.0257% and 0.0051% of iron and manganese. The high iron and manganese content in limestone is attributed to its sedimentary origin and its content of mineral and clay impurities, which increases its surface roughness and porosity. These characteristics interlock with adhesives, but they may reduce its chemical purity compared to marble

4.9. FTIR Analysis.

The FTIR spectra revealed significant changes in the 5% nanofiller samples compared with the neat polymers. For sample 3 (epoxy + 5% SiO_2 + 5% ZnO), a new peak appeared at 1,605 cm^{-1} (C=C), and the C–O band shifted from 1,183 to 1,100 cm^{-1}. These changes indicate chemical interactions between the nanoparticles and the epoxy network, together with structural crosslinking, as shown in Table 5 and Fig. 12. For sample 6 (PVAc + 5% SiO_2 + 5% ZnO), the C=O stretching frequency decreased to 1,737 cm^{-1}, the C–O band shifted to 1,022 cm^{-1}, and a new band appeared at 946 cm^{-1} (CH_2=CH) (70), as shown in Table 5 and Fig. 13. These changes suggest weakening of the ester bond and the formation of hydrogen bonds with the nanoparticles, while the main polymer backbone remained intact. Compared with the 2% nanofiller samples, the 5% formulations exhibited more pronounced spectral changes, indicating that the higher nanoparticle content produced greater interaction, better dispersion, and improved polymer–nanoparticle compatibility. The Paraloid B-72 spectrum confirmed its typical acrylic structure without new chemical interactions (71), as shown in Table 5 and Fig. 14.

5. Conclusions and Recommendations

Paraloid B-72 was used as a primer layer on the stone surface before the application of the structural adhesives. This primer acts as a protective layer that safeguards the original substrate by preventing direct contact between the adhesive and the artifact. Therefore, if the adhesive must be removed in the future, this solvent-removable layer, which can be removed using organic solvents such as acetone,

facilitates separation without causing physical or chemical damage to the underlying stone. The tested formulations showed promising mechanical performance for bonding the experimental limestone and marble specimens. Their use in archaeological conservation should be considered in conjunction with compatibility, reversibility, aging, and appearance requirements. The tests showed that adding nanofillers to epoxy strengthened all measured mechanical properties as the percentage of the additives increased. This improvement is attributed to mechanical crosslinking through the formation of a nanonetwork, particularly at the 5% concentration, which inhibits crack propagation, distributes stress, and fills voids in the polymer matrix; the force-extension curves showed that the addition of 5% nanoparticles achieved the highest shear strength and highest stiffness compared to the other samples, confirming the effectiveness of this ratio in improving the mechanical properties of the epoxy the stone surface. PVAc also exhibited improved mechanical properties following the addition of the nanofillers, although it underperformed epoxy in all mechanical tests because its interaction with the nanoparticles is physical rather than chemical. Therefore, epoxy reinforced with 5% SiO_2 and 5% ZnO exhibited the highest mechanical performance among the tested formulations. PVAc-based formulations may be considered for less demanding repairs. Paraloid B-72 should be described consistently as a removable protective barrier coating rather than as a structural adhesive because it prevents epoxy or PVAc from penetrating the stone and thereby preserves the artifact. This removable barrier coating can be dissolved using acetone or other suitable solvents. Future studies are recommended to investigate higher nanoparticle loadings, such as 7% or 10%, to determine the maximum improvement limit and to explore other nanoparticle additives, such as titanium dioxide, together with their ability to strengthen the adhesives and their economic feasibility and cost-effectiveness.

Table 1. Mechanical properties of epoxy- and PVAc-based samples 1–7.

No.	Samples	Bond Strength N/mm^2	Shear Strength MPa	Compressive Strength MPa	Tensile Strength MPa
1	Epoxy with hardener	30.481	30.057	56.3	9.25
2	Epoxy + 2% nano-SiO_2 + 2% ZnO	40.441	39.99	67.3	16.09
3	Epoxy + 5% nano-SiO_2 + 5% ZnO	45.519	46.94	86.20	20.4
4	Neat PVAc	10.10	10.34	25.9	8.2
5	PVAc + 2% nano-SiO_2 + 2% ZnO	18.318	17.289	55.9	11.21
6	PVAc + 5% nano-SiO_2 + 5% ZnO	25.244	35.90	61.4	13.21
7	Paraloid B-72 (50%)	-	8.8	-	5.26

Table 2. Physical properties of epoxy- and PVAc-based samples 1–7.

No.	Samples	Stone setting time without slipping (Min.)	Curing time hour		Viscosity
			Initial	Final	Poise
1	Epoxy with hardener	15	(2-3)	168	1.22
2	Epoxy + 2% nano-SiO_2 + 2% ZnO	15	(2-3)	168	3.51
3	Epoxy + 5% nano-SiO_2 + 5% ZnO	13	(2-3)	168	4.50
			Drying time Initial (h)	Drying time Final (h.)	
4	Neat PVAc	4	5-6	72	4.9
5	PVAc + 2% nano-SiO_2 + 2% ZnO	3	5-6	72	5.12
6	PVAc + 5% Nano SiO_2 and 5% ZnO)	2	5-6	72	5.2
7	(Paraloid B-72)	5	1-2	24	4

Table 3. Selected elemental concentrations determined by XRF (%).

No.	Samples	elements					
		Mn%	Fe%	Mg%	Na%	Si%	Ca%
1	Limestone stone	0.0103	0.1309	0.031	0.21	0.1045	37.68
2	Marble stone	0.0051	0.0279	0.034	0.22	0.0653	34.06

Table 4. Selected oxide concentrations determined by XRF (%).

No.	Samples	% oxides					
		MnO	Fe_2O_3	MgO	Na_2O	SiO_2	CaO
1	Limestone stone	0.013	0.187	0.051	0.283	0.224	52.72
2	Marble stone	0.0066	0.040	0.056	0.297	0.140	47.66

Table 5. FTIR bands of epoxy-, PVAc-, and Paraloid B-72-based samples 1–7.

No.	Samples	(FT-IR) Spectral characterisation bands (cm^{-1})			
		υ CH_2	υ C=O	υ C-O	Others
1	Epoxy with hardener	2966 2927	-	1033	υ C-H out-of-plane (732) υC=C(1605) (864-914)
2	2% Nano SiO_2 and 2% ZnO +Epoxy	2955 2918	-	1162	(864-914)
3	5% Nano SiO_2 and 5% ZnO +Epoxy	2955 2918	-	1183	υC=C (1605) υ C-H (3051)
4	Neat PVAc	3093	1755	1132	O- C=O (1206)
5	2% Nano SiO2 and 2% ZnO + PVAc	3093 2964	1735	1018	O-C=O (1212) C-O-C= (1125)
6	5% Nano SiO2 and 5% ZnO +PVAc	2921	1737	1022	C-O-C= (1118) CH_2=CH (946)
7	50% (Paraloid B-72)	2982 2951	1719	1023	C-O-C= (1138) O- C=O (1233) υ C-H 2920

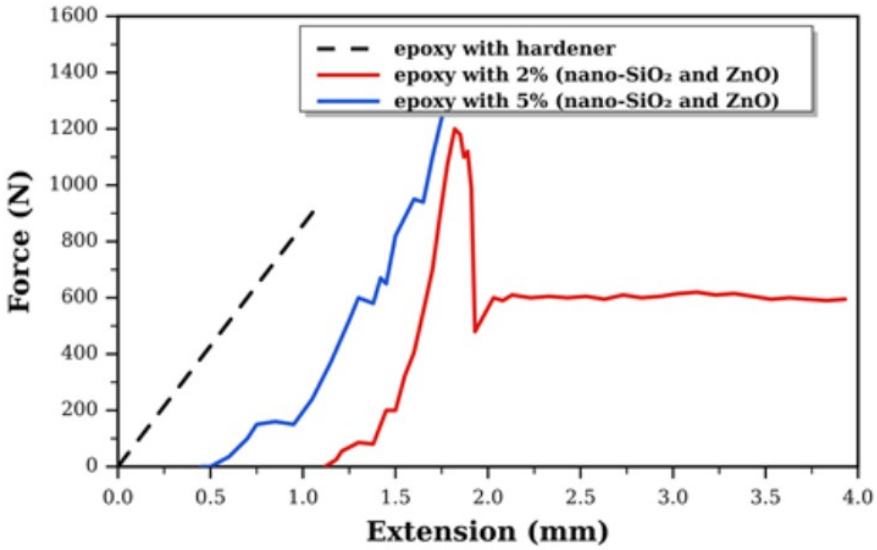

Fig. 6. Load–extension curves obtained during shear testing of neat epoxy and epoxy containing 2% or 5% each of nano-SiO_2 and ZnO.

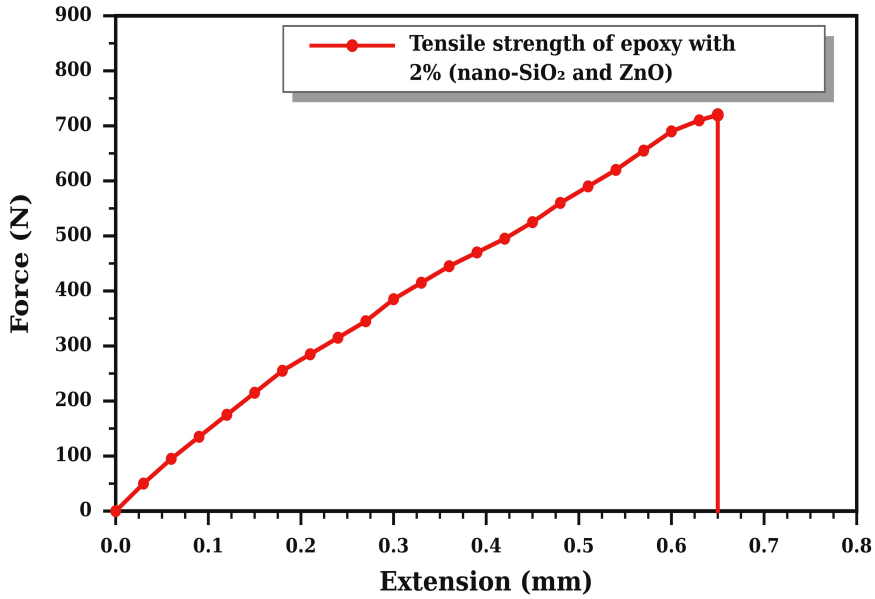

Fig. 7. Load–extension curve obtained during tensile testing of epoxy containing 2% nano-SiO_2 and 2% ZnO.

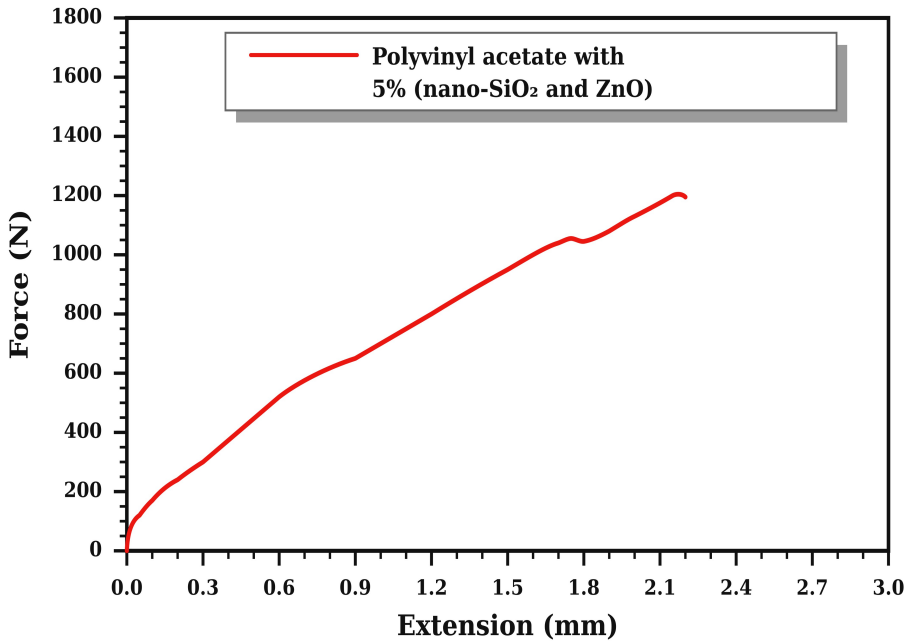

Fig. 8. Load–extension curve obtained during shear testing of PVAc containing 5% nano-SiO_2 and 5% ZnO.

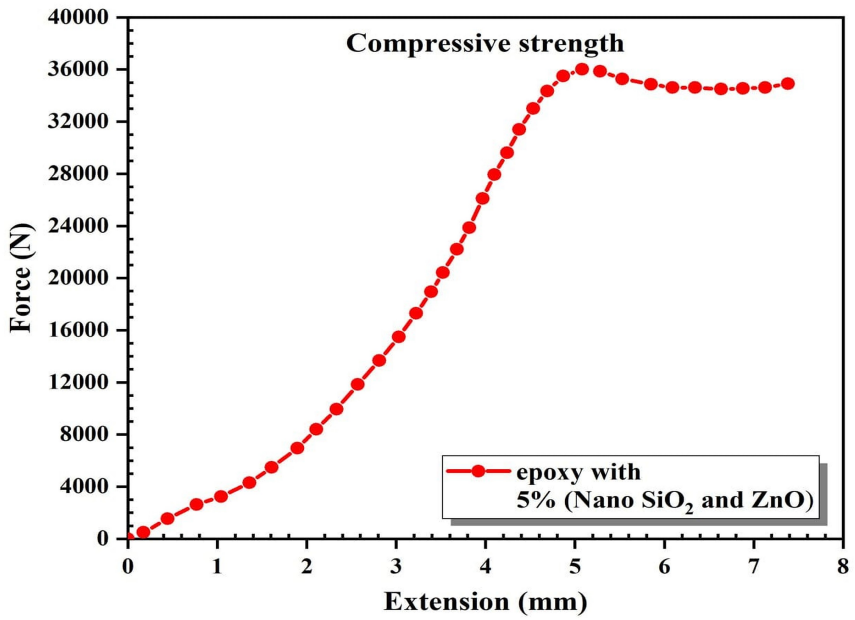

Fig. 9. Load–extension curve obtained during compressive-strength testing of epoxy containing 5% nano-SiO_2 and 5% ZnO.

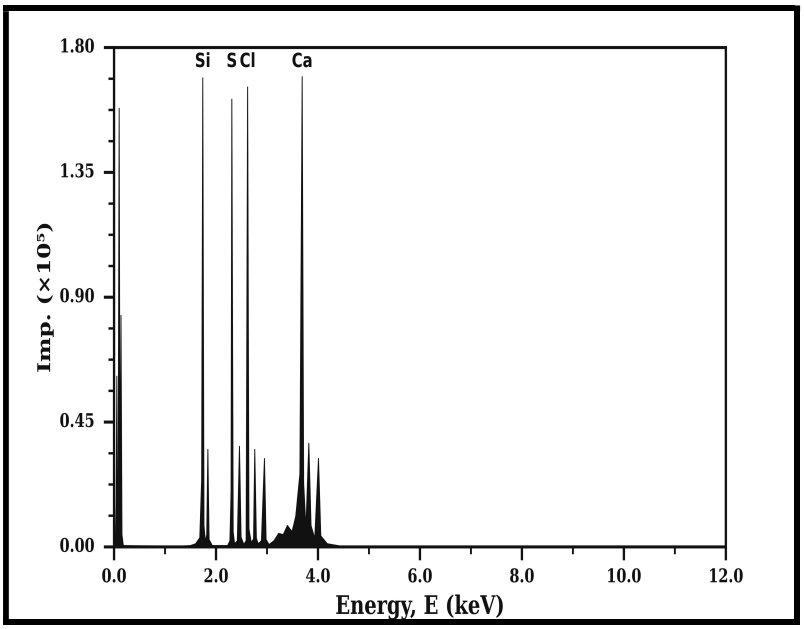

Fig. 10. X-ray fluorescence (XRF) analysis of limestone.

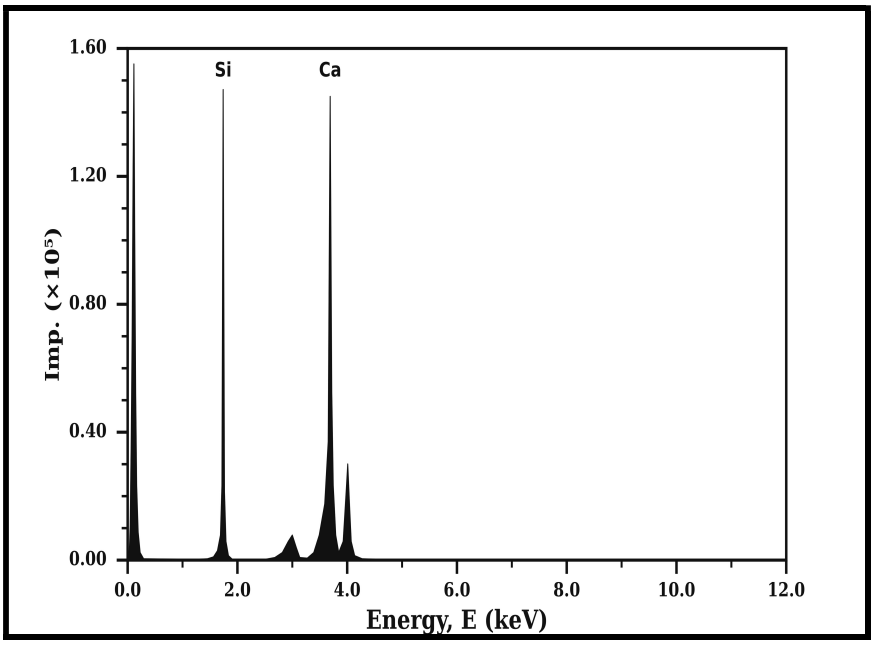

Fig. 11. X-ray fluorescence (XRF) analysis of marble.

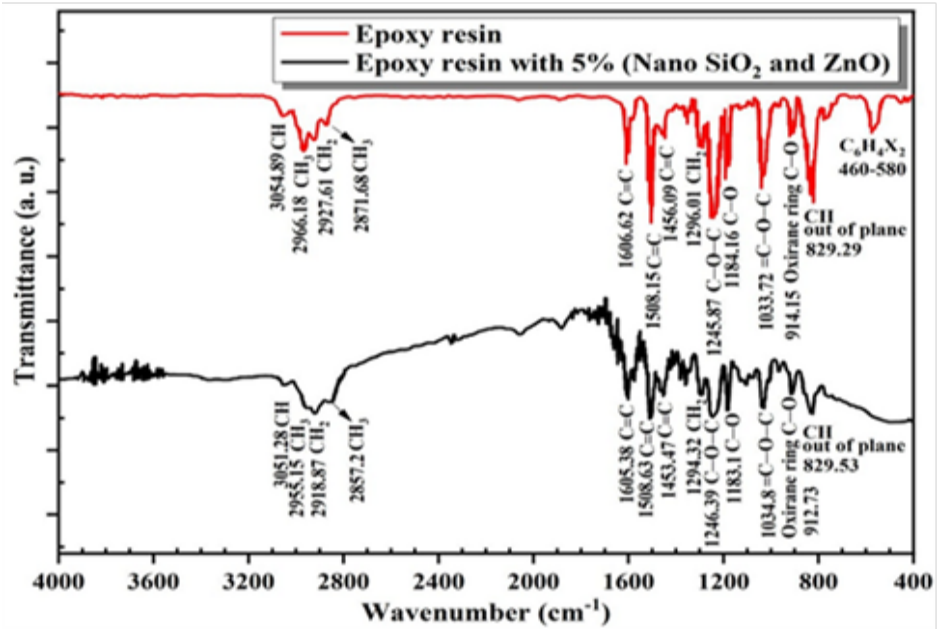

Fig. 12. FTIR spectra of neat epoxy and epoxy containing 5% nano-SiO_2 and 5% ZnO.

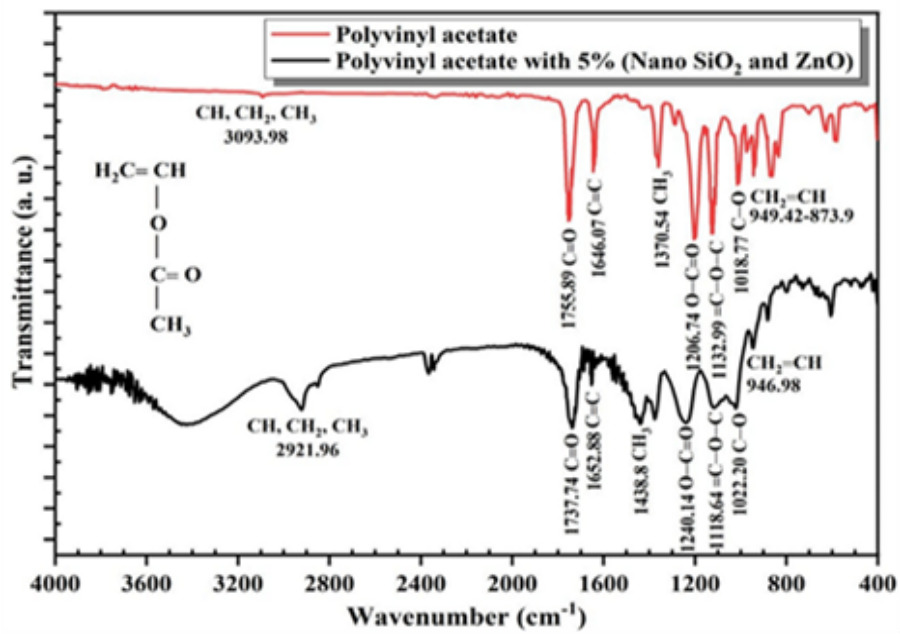

Fig. 13. FTIR spectra of neat PVAc and PVAc containing 5% nano-SiO_2 and 5% ZnO.

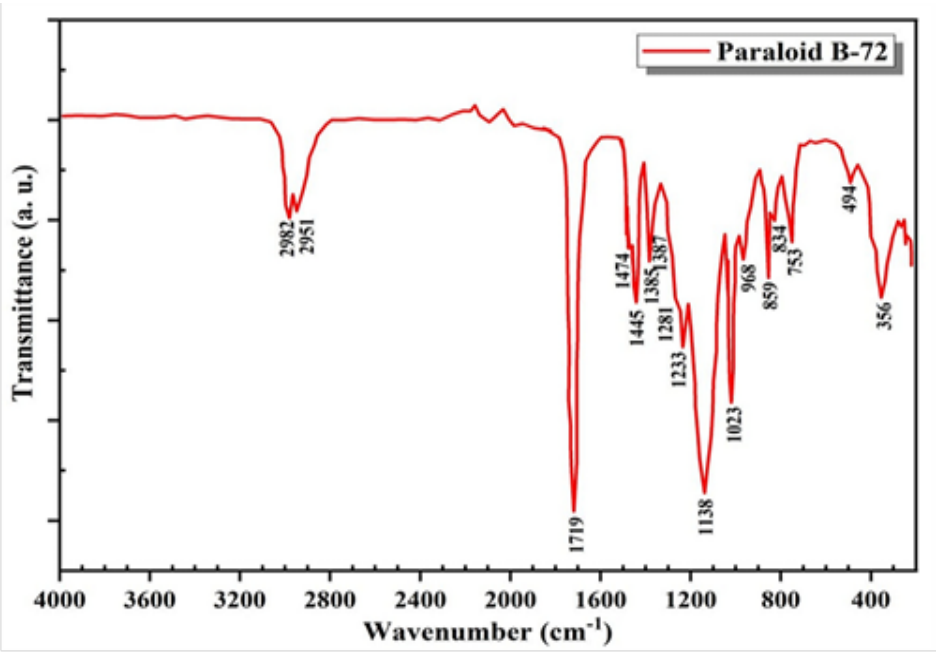

Fig. 14. FTIR spectrum of Paraloid B-72.

References

1. Hsissou, R.; Seghiri, R.; Benzekri, Z.; Hilali, M.; Rafik, M.; Elharfi, A. Polymer Composite Materials: A Comprehensive Review. *Compos. Struct.* **2021**, *262*, 113640. https://doi.org/10.1016/j.compstruct.2021.113640

2. Bhong, M.; Khan, T.K.H.; Devade, K.; Vijay Krishna, B.; Sura, S.; Eftikhaar, H.K.; Pal Thethi, H.; Gupta, N. Review of Composite Materials and Applications. *Mater. Today Proc.* 2023. https://doi.org/10.1016/j.matpr.2023.10.026

3. Fan, Q.; Duan, H.; Xing, X. A Review of Composite Materials for Enhancing Support, Flexibility and Strength in Exercise. *Alex. Eng. J.* **2024**, *94*, 90–103. [Google Scholar] https://doi.org/10.1016/j.aej.2024.03.048

4. KHADEMI, Davoud, et al. Mechanical property improvement of epoxy composites via electrospun SiO2 nanofibers. *The International Journal of Advanced Manufacturing Technology*, 2026, 1-22. https://doi.org/10.21203/rs.3.rs-8186752/v1

5. Upadhyaya S, Devi M, Borah S, Sarma NS. Organic polymers for adhesive applications: history, progress, and the future. Organic Polymers in Energy-Environmental Applications. 2024 Nov 4:491-512. https://doi.org/10.1002/9783527842810.ch22

6. Dinte E, Sylvester B. Adhesives: applications and recent advances. Applied adhesive bonding in science and technology. 2018 Feb 21:119-34. https://doi.org/10.5772/intechopen.71854

7. Chanakyan C, Ashok Raj R, Vinoth Kumar H, Mathiyalagan P. Synthesis and characterisation of glass fibre with hybrid nano ceramic particles reinforced polymer composites for aerospace applications. Canadian Metallurgical Quarterly. 2026 Apr 3;65(2):1311-41. https://doi.org/10.1080/00084433.2025.2511506

8. DONI, Mihaela; FIERASCU, Irina; FIERASCU, Radu Claudiu. Recent developments in materials science for the conservation and restoration of historic artifacts. Applied Sciences, 2024, 14.23: 11363. https://doi.org/10.3390/app142311363

9. Tang Z, Liu X, Feng X. Research Progress on Epoxy Resins in Cultural Heritage Conservation. Polymers. 2025 Jun 24;17(13):1747 https://doi.org/10.3390/polym17131747

10. Chen Z, Liu X, Chen H, Li J, Wang X, Zhu J. Application of epoxy resin in cultural relics protection. Chinese Chemical Letters. 2024 Apr 1;35(4):109194. https://doi.org/10.1016/j.cclet.2023.109194

11. Zhou Y, Zhao ZH, Zeng Y, Tian S, Sun F, Cheng Y, Li Y, Fu Z, Fu J. Ultra-Robust and Tough Epoxy Resin Enabled by Pulley Mechanism-Based Curing Agent for Strong and Reversible Adhesion. Advanced Functional Materials. 2025 Nov;35(46):e1705https://doi.org/10.1002/adfm.202517052

12. Jin FL, Li X, Park SJ. Synthesis and application of epoxy resins: A review. Journal of industrial and engineering chemistry. 2015 Sep 25;29:1-1. https://doi.org/10.1016/j.jiec.2015.03.026

13. Aldosari MA, Darwish SS, Adam MA, Elmarzugi NA, Ahmed SM. Re-Assembly of archaeological massive limestones using epoxy resin modified with nanomaterials—part 1: experimental. Green and Sustainable Chemistry. 2020;10(1):24-38. https://doi.org/10.4236/gsc.2020.101003

14. Sukanto H, Raharjo WW, Ariawan D, Triyono J, Kaavesina M. Epoxy resins thermosetting for mechanical engineering. Open Engineering. 2021 Jul 12;11(1):797-814. https://doi.org/10.1515/eng-2021-0078

15. Mi X, Liang N, Xu H, Wu J, Jiang Y, Nie B, Zhang D. Toughness and its mechanisms in epoxy resins. Progress in Materials Science. 2022 Oct 1;130:100977. https://doi.org/10.1016/j.pmatsci.2022.100977

16. Abiodun MI, Oluwole OI, Damilola AA, Ondieki BA, Ibrahim MA. Applications of Epoxy Resin: Adhesives, Coatings, and Composites. Epoxy-Materials, Applications and Advanced Technologies 2025 Oct 2. Intech Open. DOI: 10.5772/intechopen.1012261

17. Danchenko Y, Andronov V, Skripinets A, Kosse A, Volnyanko E. Decorative-protective epoxy compositions for the restoration of natural stone. In AIP Conference Proceedings 2023 Dec 7 (Vol. 2490, No. 1, p. 050015). AIP Publishing LLC. **https://doi.org/10.1063/5.0142212**

18. Nagraik P, Shukla SR, Kelkar BU. Enhancing poplar-wood properties through nano-silica fortified polyvinyl-acetate impregnation. Wood Material Science & Engineering. 2025 Jan 2;20(1):191-204. https://doi.org/10.1080/17480272.2024.2337150

19. Hong W, Meng M, Xie J, Gao D, Xian M, Wen S, Huang S, Kang C. Properties and thermal analysis study of modified polyvinyl acetate (PVA) adhesive. Journal of Adhesion Science and Technology. 2018 Oct 2;32(19):2180-94. https://doi.org/10.1080/01694243.2018.1465687

20. Petković G, Vukoje M, Bota J, Pasanec Preprotić S. Enhancement of polyvinyl acetate (PVAc) adhesion performance by SiO2 and TiO2 nanoparticles. Coatings. 2019 Oct 30;9(11):707. https://doi.org/10.3390/coatings9110707

21. Bardak T, Tankut AN, Tankut N, Sozen E, Aydemir D. The effect of nano-TiO2 and SiO2 on bonding strength and structural properties of poly (vinyl acetate) composites. Measurement. 2016 Nov 1;93:80-5. https://doi.org/10.1016/j.measurement.2016.07.004

22. Muhammad, U.L.; Musa, M.Y.; Yusuf, U.; Nasir, A.B. Limestone as Solid Mineral to Develop National Economy. *Am. J. Phys. Chem.* **2018**, *7*(2), 23–28. https://doi.org/10.11648/j.ajpc.20180702.13

23. SANDSTRÖM, Karin, et al. Characterization of limestone surface impurities and resulting quicklime quality. Minerals, 2024, 14.6: 608. https://doi.org/10.3390/min14060608

24. Qi G, Wang D, Xu D, Zhang D, Wang Q, Tang Y, Zhu Y. Analysis of lime paste and bricks from the Ming Dynasty: Composition, structure, properties, and adhesion mechanism. Construction and Building Materials. 2025 Jan 31;461:139929. https://doi.org/10.1016/j.conbuildmat.2025.139929

25. Ali AH, Hamood AA, Anoon IA. Evaluation of mechanical properties of Iraqi limestone ore. In AIP Conference Proceedings 2025 Mar 31 (Vol. 3303, No. 1, p. 060024). AIP Publishing LLC. https://doi.org/10.1063/5.0263313

26. Mani M. Silica nanoparticle-enhanced mechanical properties and energy absorption behavior of hybrid fiber-reinforced polymer composites for structural applications. Next Materials. 2025 Oct 1;9:101213. https://doi.org/10.1016/j.nxmate.2025.101213

27. Gherardi F, Maravelaki PN. Advances in the application of nanomaterials for natural stone conservation. RILEM Technical Letters. 2022 Aug 10;7:20-9. https://doi.org/10.21809/rilemtechlett.2022.159

28. Najafianashrafi M, Moradpour P, Jahan Latibari A, Edalat H. Adhesive modification and improvement of properties of polyvinyl acetate using nano silica. Iranian Journal of Wood and Paper Science Research. 2023 Jun 22;38(2):128-40. https://doi.org/10.22092/ijwpr.2023.361007.1743

29.KHADEMI, Davoud, et al. Mechanical property improvement of epoxy composites via electrospun SiO2 nanofibers. The International Journal of Advanced Manufacturing Technology, 2026, 143.1: 677-698. https://doi.org/10.1007/s00170-026-17568-x

30. TANKUT, Nurgul, et al. The effect of different nanoparticles and open time on bonding strength of poly (vinyl acetate) adhesive. *Measurement*, 2016, 81: 80-84. http://dx.doi.org/10.1016/j.measurement.2015.12.003

31. Tee ZY, Yeap SP, Hassan CS, Kiew PL. Nano and non-nano fillers in **enhancing** mechanical properties of epoxy resins: a brief review. Polymer-Plastics Technology and Materials. 2022 May 3;61(7):709-25. https://doi.org/10.1080/25740881.2021.2015778

32. Aldosari MA, Darwish SS, Adam MA, Elmarzugi NA, Ahmed SM. Using ZnO nanoparticles in fungal inhibition and self-protection of exposed marble columns in historic sites. Archaeological and Anthropological Sciences. 2019 Jul 1;11(7):3407-22. https://doi.org/10.1007/s12520-018-0762-z

33. Mirmohammadi SM, Moini Jazani O, Gharieh A. Thermomechanical analyses and ANN modeling of novel epoxy adhesives with CSR particles and zinc oxide nanoparticles in structural bonding. Scientific Reports. 2025 Apr 2;15(1):11201. https://doi.org/10.1038/s41598-025-96270-6

34.ALAM, Mohammad Asif, et al. Effects of SiO2 and ZnO nanoparticles on epoxy coatings and their performance investigation using thermal and nanoindentation techniques. Polymers, 2021, 13.9: 1490. https://doi.org/10.3390/polym13091490

35. IBRAHIM, Shimaa, et al. Biodegradation of Synthetic Polymers Used in Consolidation of Deteriorated Limestone Monuments. *Polymers*, 2026, 18.10: 1218. https://doi.org/10.3390/polym18101218

36. Sharma, D. K., Shukla, S., Sharma, K. K., & Kumar, V. (2022). A review on ZnO: 515 Fundamental properties and applications. Materials Today: Proceedings, 49, 3028-3035. 516 https://doi.org/10.1016/j.matpr.2020.10.238.

37.Kaplan Z, Böke H, Sofuoğlu A, İpekoğlu B. Long-term stability of biodegradable polymers on building limestone. Progress in Organic Coatings. 2019 Jun 1;131:378-88. https://doi.org/10.1016/j.porgcoat.2019.03.004

38. Vinçotte A, Beauvoit E, Boyard N, Guilminot E. Effect of solvent on PARALOID® B72 and B44 acrylic resins used as adhesives in conservation. Heritage Science. 2019 Jun 25;7(1):1-9. https://doi.org/10.1186/s40494-019-0283-9

39.Musacchi J, Silva HM, Cabral-Fonseca S, Esteves L, Delgado Rodrigues J, Rodrigues MP, Pereira SR. Adhesion of historic tile fragments in outdoor architectural settings. Buildings. 2024 Feb 1;14(2):375. https://doi.org/10.3390/buildings14020375

40. Sabatini V, Cattò C, Cappelletti G, Cappitelli F, Antenucci S, Farina H, Ortenzi MA, Camazzola S, Di Silvestro G. Protective features, durability and biodegradation study of acrylic and methacrylic fluorinated polymer coatings for marble protection. Progress in Organic Coatings. 2018 Jan 1;114:47-57.https://doi.org/10.1016/j.porgcoat.2017.10.003

41. TANG, Zirui; LIU, Xinyou; FENG, Xinhao. Research progress on epoxy resins in cultural heritage conservation. Polymers, 2025, 17.13: 1747. https://doi.org/10.3390/polym17131747

42. Ershad-Langroudi A. Protective material coatings for preserving cultural heritage monuments and artwork. Bentham Science Publishers; 2022 Apr 11.https://doi.org/10.2174/9789815049046122010 1

43. Zhao X, Li X, Zhang S, Niu Q, Li Z, Xue C. Investigation of whitening mechanism on cultural relic surfaces treated with Paraloid B72. Coatings. 2024 Sep 26;14(10):1240. https://doi.org/10.3390/coatings14101240

44. McCoy JD, Ancipink WB, Clarkson CM, Kropka JM, Celina MC, Giron NH, Hailesilassie L, Fredj N. Cure mechanisms of diglycidyl ether of bisphenol A (DGEBA) epoxy with diethanolamine. Polymer. 2016 Nov 22;105:243-54. https://doi.org/10.1016/j.polymer.2016.10.028

45. Arif, M.; Ktit, H.; Melin, K.; Chakraborty, C.; Ceccherini, S.; Sapkota, J.; Layek, R. Sulfanilic Acid-Functionalized Kraft Lignin as a Multifunctional Additive for Poly(vinyl acetate)-Based Wood Adhesives and Composite Film Applications. Biomass Bioenergy 2027, 216, 109764. https://doi.org/10.1016/j.biombioe.2026.109764

46. Ntelia E, Karapanagiotis I. Superhydrophobic Paraloid B72. Progress in Organic Coatings. 2020 Feb 1;139:105224. https://doi.org/10.1016/j.porgcoat.2019.105224
47.
47. Musa AA, Bello A, Adams SM, Onwualu AP, Anye VC, Bello KA, Obianyo II. Nano-enhanced polymer composite materials: a review of current advancements and challenges. Polymers. 2025 Mar 26;17(7):893.https://doi.org/10.3390/polym17070893

48. DEMIRAL, Murat. Strength in adhesion: A multi-mechanics review covering tensile, shear, fracture, fatigue, creep, and impact behavior of polymer bonding in composites. *Polymers*, 2025, 17.19: 2600. https://doi.org/10.3390/polym17192600

49.ABDELHADY, Saleh S., et al. Enhancement of Epoxy-derived Polymer Nanocomposites Strengthened with Titanium Dioxide (TiO2) and Silicon Oxide (SiO2) Nanoparticles. Silicon, 2026, 1-15. https://doi.org/10.1007/s12633-026-03667-7

50. Kara Y, Acar V, Seydibeyoglu MO. Mechanical properties of nanoparticle-based polymer composites. In Nanoparticle-based polymer composites 2022 Jan 1 (pp. 95-108). Woodhead Publishing. https://doi.org/10.1016/B978-0-12-824272-8.00007-5

51. Kontou E, Christopoulos A, Koralli P, Mouzakis DE. The effect of silica particle size on the mechanical enhancement of polymer nanocomposites. Nanomaterials. 2023 Mar 18;13(6):1095. **https://doi.org/10.3390/nano13061095**

52. NTELIA, Eleni; KARAPANAGIOTIS, Ioannis. Super hydrophobic Paraloid B72. *Progress in Organic Coatings*, 2020, 139: 105224. https://doi.org/10.1016/j.porgcoat.2019.105224

53. LI, Hongwei, et al. Recent research progress and advanced applications of silica/polymer nanocomposites. *Nanotechnology Reviews*, 2022, 11.1: 2928-2964. **https://doi.org/10.1515/ntrev-2022-0484**

54. Zhang J, Zhang Z, Huang R, Tan L. Advances in toughening modification methods for epoxy resins: A comprehensive review. Polymers. 2025 May 7;17(9):1288. https://doi.org/10.3390/polym17091288

55.YAMAZAKI, Taiga, et al. Experimental investigation of adhesive joint strength and stress-based criteria under tensile/compression–shear stress state using a developed fixture. *The Journal of Adhesion*, 2026, 102.3: 179-200. https://doi.org/10.1080/00218464.2025.2528923

56. Qadir WM, Al Zahawi SK, Mohammed AS. Comprehensive review of tile adhesives: Slip, bond strength, chemical composition, and microstructural insights. Case Studies in Construction Materials. 2025 Jul 1;22: e04634. **https://doi.org/10.1016/j.cscm.2025.e04634**

57. EL OMARI, Mohamed, et al. Spectroscopic characterization of limestone and dolostone by Raman, FTIR, XRD and XRF Analyses. In: E3S Web of Conferences. EDP Sciences, 2025. p. 01007. https://doi.org/10.1051/e3sconf/202567501007

58. Godts, S., Orr, S.A., Steiger, M., Stahlbuhk, A., De Kock, T., Desarnaud, J., De Clercq, H., & Cnudde, V. Salt mixtures in stone weathering. *Scientific Reports*, 2023, *13*(1), 13306. https://doi.org/10.1038/s41598-023-40590-y

59. IBRAHIM, Mohamed Moustafa; MOHAMED, Wael Sabry; MOHAMED, Hamdy Mohamed. Experimental study for evaluation of Paraloid® B72 and its nanocomposite with nano TiO2 and nano ZnO for consolidation of pottery samples. *Scientific Culture*, 2021, 7.2: 101-111 https://creativecommons.org/licenses/by/4.0/

60. Budzik, M.K.; Wolfahrt, M.; Reis, P.; et al. Testing mechanical performance of adhesively bonded composite joints in engineering applications: An overview. J. Adhes. 2022, 98, 2133–2209. https://doi.org/10.1080/00218464.2021.1953479.

61.SARAVANA KUMAR, M., et al. Optimizing the filler distribution to enhance the interlaminar shear strength and impact resistance of fiber-reinforced epoxy composites. *Polymer Composites*, 2025, 46.14: 12650-12662. https://doi.org/10.1002/pc.29885

62. BURHAN, Salsabeel Kareem, et al. Predicting Stress–Strain Behavior of Silica–Epoxy Nanocomposites Using Random Forest Regression. *Journal of Composites Science*, 2025, 9.11: 619..https://doi.org/10.3390/jcs9110619

63. YAHYAA, Mohammed M.; ALEABI, Suad H. Enhancing Some Mechanical Properties (Compression, Impact, Hardness, Young modulus) and Thermal Conductivity, Diffusion Coefficient of Micro Epoxy Composites. *Ibn AL-Haitham Journal For Pure and Applied Sciences*, 2022, 35.3: 32-43. https://doi.org/10.30526/35.3.2841

64. EL OMARI, Mohamed, et al. Spectroscopic characterization of limestone and dolostone by Raman, FTIR, XRD and XRF Analyses. In: *E3S Web of Conferences*. EDP Sciences, 2025. p. 01007. **https://doi.org/10.1051/e3sconf/202567501007**

65. LONG, Jiejie; LI, Chuanxi; LI, You. Enhancement of mechanical and bond properties of epoxy adhesives modified by SiO2 nanoparticles with active groups. Polymers, 2022, 14.10: https://doi.org/10.3390/polym14102052

66. PETKOVIĆ, Gorana, et al. Impact of SiO2 and TiO2 nanoparticles on the elasticity and aging resistance of polyvinyl acetate (PVAc) adhesive. *Materials*, 2024, 17.23: 5957. https://www.mdpi.com/1996-1944/17/23/5957#

67. Raja, T., Devarajan, Y., & Kailiappan, N. Study on enhancing mechanical and thermal properties of carbon fiber reinforced epoxy composite through zinc oxide nanofiller. Discov Appl Sci 6, 566 (2024). https://doi.org/10.1007/s42452024-06270-w

68. ABDEL-RAHIM, Ruaa Haitham; ATTALLAH, Marwah Subhi; MOHAMMED, Reem Alaa. Investigation of the effect of nano silica dioxide additives on the properties of epoxy resin for use in industrial applications. In: Materials Science Forum. Trans Tech Publications Ltd, 2022. p. 103-113. https://doi.org/10.4028/www.scientific.net/MSF.1050.103

69. BHORE, Nishant; THORAT, Prashant; DESHMUKH, Mangesh. Enhancing epoxy nanocomposites with mineral nanofillers: A comprehensive review of particle size, shape, and concentration. *Zastita Materijala*, 2026, 67.2: 352-372. https://doi.org/10.62638/ZasMat1554

70. PETKOVIĆ, Gorana, et al. Enhancement of polyvinyl acetate (PVAc) adhesion performance by SiO2 and TiO2 nanoparticles. Coatings, 2019, 9.11: 707. https://doi.org/10.3390/coatings9110707

71. GKRAVA, Eirini, et al. Superhydrophobic Nanocomposite of Paraloid B72 and Modified Calcium Carbonate Nanoparticles for Cultural Heritage Conservation. Coatings, 2026, 16.3: 347. https://doi.org/10.3390/coatings16030347